ATP-induced conformational changes of the nucleotide-binding domain of Na,K-ATPase

Mark Hilge[1,5], Gregg Siegal[1], Geerten W Vuister[2], Peter Güntert[3], Sergio M Gloor[4] & Jan Pieter Abrahams[1]

The Na,K-ATPase hydrolyzes ATP to drive the coupled extrusion and uptake of Na$^+$ and K$^+$ ions across the plasma membrane. Here, we report two high-resolution NMR structures of the 213-residue nucleotide-binding domain of rat α1 Na,K-ATPase, determined in the absence and the presence of ATP. The nucleotide binds in the *anti* conformation and shows a relative paucity of interactions with the protein, reflecting the low-affinity ATP-binding state. Binding of ATP induces substantial conformational changes in the binding pocket and in residues located in the hinge region connecting the N- and P-domains. Structural comparison with the Ca-ATPase stabilized by the inhibitor thapsigargin, E2(TG), and the model of the H-ATPase in the E1 form suggests that the observed changes may trigger the series of events necessary for the release of the K$^+$ ions and/or disengagement of the A-domain, leading to the eventual transfer of the γ-phosphate group to the invariant Asp369.

The electrochemical gradient of Na$^+$ and K$^+$ ions across the plasma membrane, established by the Na,K-ATPase or sodium pump, is essential for cellular function[1,2]. The Na,K-ATPase belongs to family II P-type ATPases that transport the abundant ions Ca^{2+} and Na$^+$ in exchange for H$^+$ or K$^+$. The sodium pump is composed of a catalytic α subunit, common to all P-type ATPases, and a regulatory β subunit that is unique to Na,K- and H,K-ATPases. A substantial body of biochemical research has identified the major steps in the ion pumping cycle of the P-type ATPases. In the Post-Albers scheme[3] of this cycle (**Fig. 1a**), ATP initially binds with a low apparent affinity (K_d ~200–400 μM) in the E2[2K] conformation. With the release of the K$^+$ ions, the affinity of Na,K-ATPase for ATP increases dramatically (K_d ~30–100 nM). Upon binding of three Na$^+$ ions, the sodium pump adopts the E1ATP[3Na] state in which phosphorylation of the invariant Asp369 takes place (for a more detailed description of the pump cycle, see refs. 4,5).

Understanding of the molecular mechanism of the P-type ATPases requires high-resolution, three-dimensional structures of the enzymes at various points in the pump cycle. Two such structures have recently become available for the Ca-ATPase of sarcoplasmic reticulum (SERCA1a) in the E1 (PDB entry 1EUL)[6] and E2 (PDB entry 1IWO)[7] state. These structures reveal that the Ca-ATPase consists of a transmembrane domain (TM) of 10 α-helices, an N-domain that binds ATP, a P-domain containing the invariant aspartate located at the bottom of a shallow cavity and an anchor or A-domain. In the E1 state of Ca-ATPase, two Ca^{2+} ions are bound at the ion-binding sites in the TM domain (E1[2Ca]), whereas the E2 state is stabilized by the inhibitor thapsigargin (E2(TG)). Notably, the A-domain is in contact with the N- and P-domains in the E2 state but disengaged in the E1 state. In addition to the X-ray diffraction structures, lower-resolution electron microscopy (EM)–based structures of the Ca-ATPase[8,9], the Na,K-ATPase[10,11] and the H-ATPase[12] are available in a variety of different conformations.

Sequence analysis (http://www.biobase.dk/~axe/Patbase.html) and electron microscopy structure comparison[8–12] suggest that all P-type ATPases share the same overall fold and, in conjunction with the biochemical data, exhibit strong mechanistic similarities. However, there is no high-resolution structural data for the Na,K-ATPases in general and no data for the ATP-bound form of any P-type ATPase. Because the binding of ATP is an essential event in the pumping cycle, we were interested in exploring its structural consequences. Here, we report ensembles of solution structures for the N-domain of rat α1 Na,K-ATPase (NaKα1) in its native and ATP-bound forms. Our data show that a conformational change occurs in the hinge region connecting the N- and P-domains that is likely to be relevant for subsequent steps of the reaction cycle.

RESULTS

Structure description

We determined the structures of the native and ATP-bound N-domain of NaKα1 (residues Gln376–Pro588) using high-resolution, heteronuclear, multidimensional NMR spectroscopy. The domain has the topology of a twisted, six-stranded, antiparallel β-sheet that is flanked by two α-helices on either side (**Fig. 1b**). The structures are well defined by the NMR data, with r.m.s. deviations for the backbone atoms of 0.97 Å (native) and 1.00 Å (ATP-bound) for the ordered

[1]Leiden Institute of Chemistry, Gorlaeus Laboratories, Leiden University, P.O. Box 9502, 2300 RA Leiden, The Netherlands. [2]Department of Biophysical Chemistry, NSRIM Center, University of Nijmegen, Toernooiveld 1, 6525 ED Nijmegen, The Netherlands. [3]RIKEN Genomic Sciences Center, C112, 1-7-22 Suehiro, Tsurumi, Yokohama 230-0045, Japan. [4]Institute of Biochemistry, University of Zürich, Winterthurerstr. 190, 8057 Zürich, Switzerland. [5]Present address: Department of Biophysical Chemistry, NSRIM Center, University of Nijmegen, Toernooiveld 1, 6525 ED Nijmegen, The Netherlands. Correspondence should be addressed to M.H. (hilge@nmr.kun.nl).
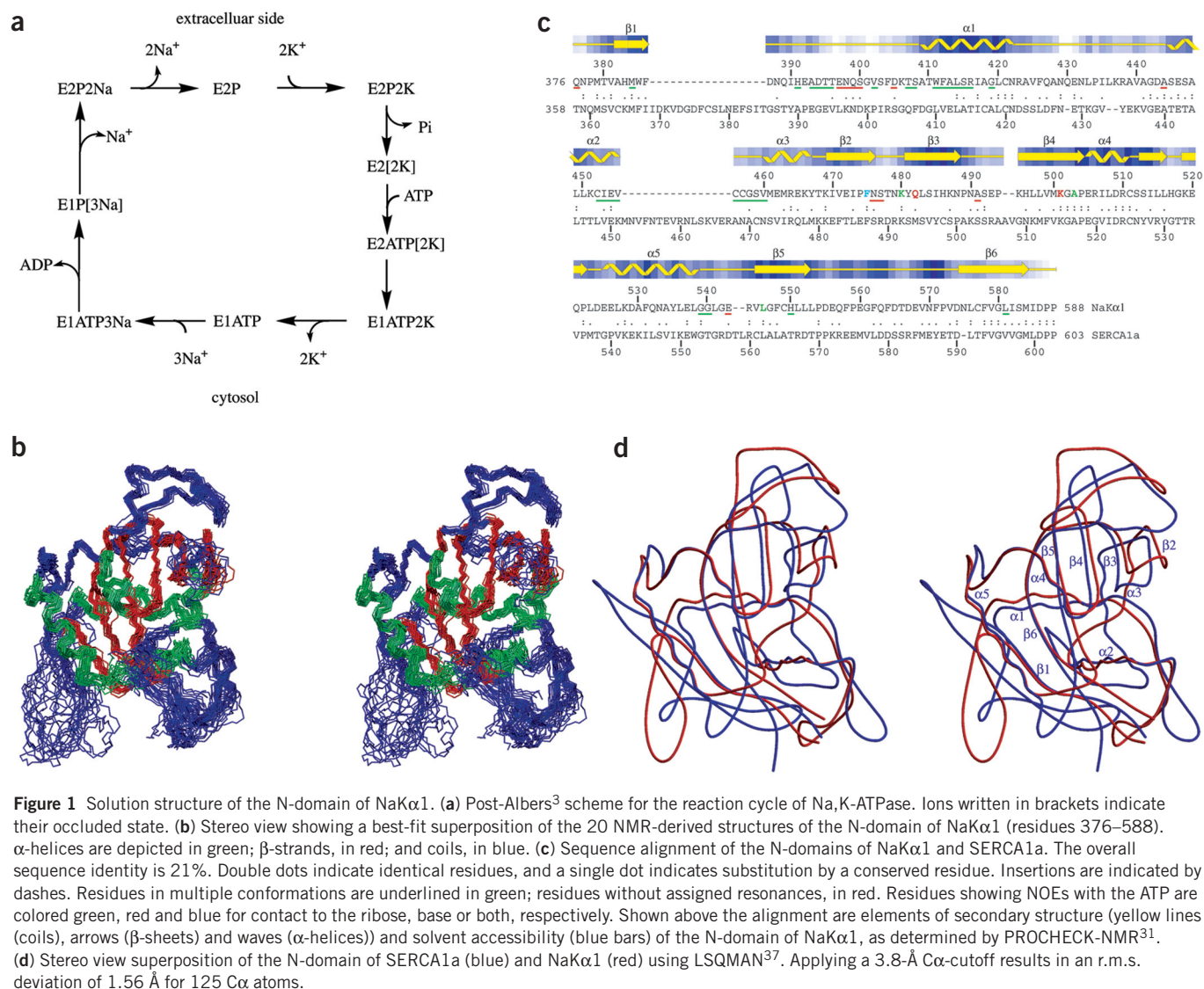
Figure 1 Solution structure of the N-domain of NaKα1. (**a**) Post-Albers[3] scheme for the reaction cycle of Na,K-ATPase. Ions written in brackets indicate their occluded state. (**b**) Stereo view showing a best-fit superposition of the 20 NMR-derived structures of the N-domain of NaKα1 (residues 376–588). α-helices are depicted in green; β-strands, in red; and coils, in blue. (**c**) Sequence alignment of the N-domains of NaKα1 and SERCA1a. The overall sequence identity is 21%. Double dots indicate identical residues, and a single dot indicates substitution by a conserved residue. Insertions are indicated by dashes. Residues in multiple conformations are underlined in green; residues without assigned resonances, in red. Residues showing NOEs with the ATP are colored green, red and blue for contact to the ribose, base or both, respectively. Shown above the alignment are elements of secondary structure (yellow lines (coils), arrows (β-sheets) and waves (α-helices)) and solvent accessibility (blue bars) of the N-domain of NaKα1, as determined by PROCHECK-NMR[31]. (**d**) Stereo view superposition of the N-domain of SERCA1a (blue) and NaKα1 (red) using LSQMAN[37]. Applying a 3.8-Å Cα-cutoff results in an r.m.s. deviation of 1.56 Å for 125 Cα atoms.

regions (**Table 1**). In the native protein, 29 residues, or 14% of the molecule, displayed multiple peaks in the NMR spectra (**Fig. 1c**), indicating slow exchange between two or more conformations. No resonances were observed for 11 residues.

The overall fold of the N-domain of NaKα1 is similar to that of the N-domain of SERCA1a (**Fig. 1d**). Structural differences mainly occur where SERCA1a has large inserts relative to NaKα1. The cluster of aromatic residues formed by Phe558, Phe562, Phe564 and Phe571 in NaKα1 is part of a scaffold covering the majority of the central β-sheet. The analogous portion of the Ca-ATPase is rotated by ~60° relative to NaKα1 and, with the exception of Tyr587, lacks the aromatic residues. In SERCA2a, the cardiac isoform of the Ca-ATPase, residues Lys397–Val402 are thought to interact with the unphosphorylated form of the regulator phospholamban[13]. On the basis of sequence alignments, this region was believed to be missing in the sodium pump. However, in the structure of NaKα1, residues Ala393–Thr407 form a largely disordered, solvent-accessible loop that occupies a position similar to the phospholamban interaction site in the Ca-ATPase. Therefore, this region in the Na,K-ATPase may also interact with an as-yet-unidentified regulator molecule.

The ATP-binding pocket and substrate binding

To gain insight into the structural effects of nucleotide binding, we first titrated ATP, ADP and MgATP into samples of either [15]N- or ^{13}C,[15]N-labeled N-domain and monitored binding by perturbation of peaks in the [^{1}H,^{15}N]-HSQC spectrum. For all three substrates, we observed a gradual shift of the protein resonances, indicating that the nucleotides are in rapid exchange on the NMR time scale. Fitting of the data (**Fig. 2a**) demonstrates that ATP binds weakly to the isolated N-domain (K_d ~5 mM). Biochemical experiments showed that the apparent affinity of the intact Na,K-ATPase in the E2 state is in a similar range (K_d ~0.2–0.4 mM)[14]. However, unlike other cation pumps, Na,K-ATPase can bind free ATP with high affinity (K_d ~30–100 nM) in Mg^{2+}-free, EDTA-containing buffer[14]. Compared with ATP, titration with MgATP yields a substantially reduced affinity (K_d ~25 mM) for the N-domain (**Fig. 2a**).

At the endpoint of the ATP titration, a significant number of residues (43 of 201) showed chemical shift changes >0.05 p.p.m. in the amide proton and >0.3 p.p.m. in the ^{15}N dimensions. ADP binds to the N-domain with significantly lower affinity, with a K_d of ~25 mM (**Fig. 2a**). As a result, the number of [^{1}H,^{15}N]-HSQC peaks with large shifts is reduced to 12, suggesting that the γ-phosphate group of ATP is
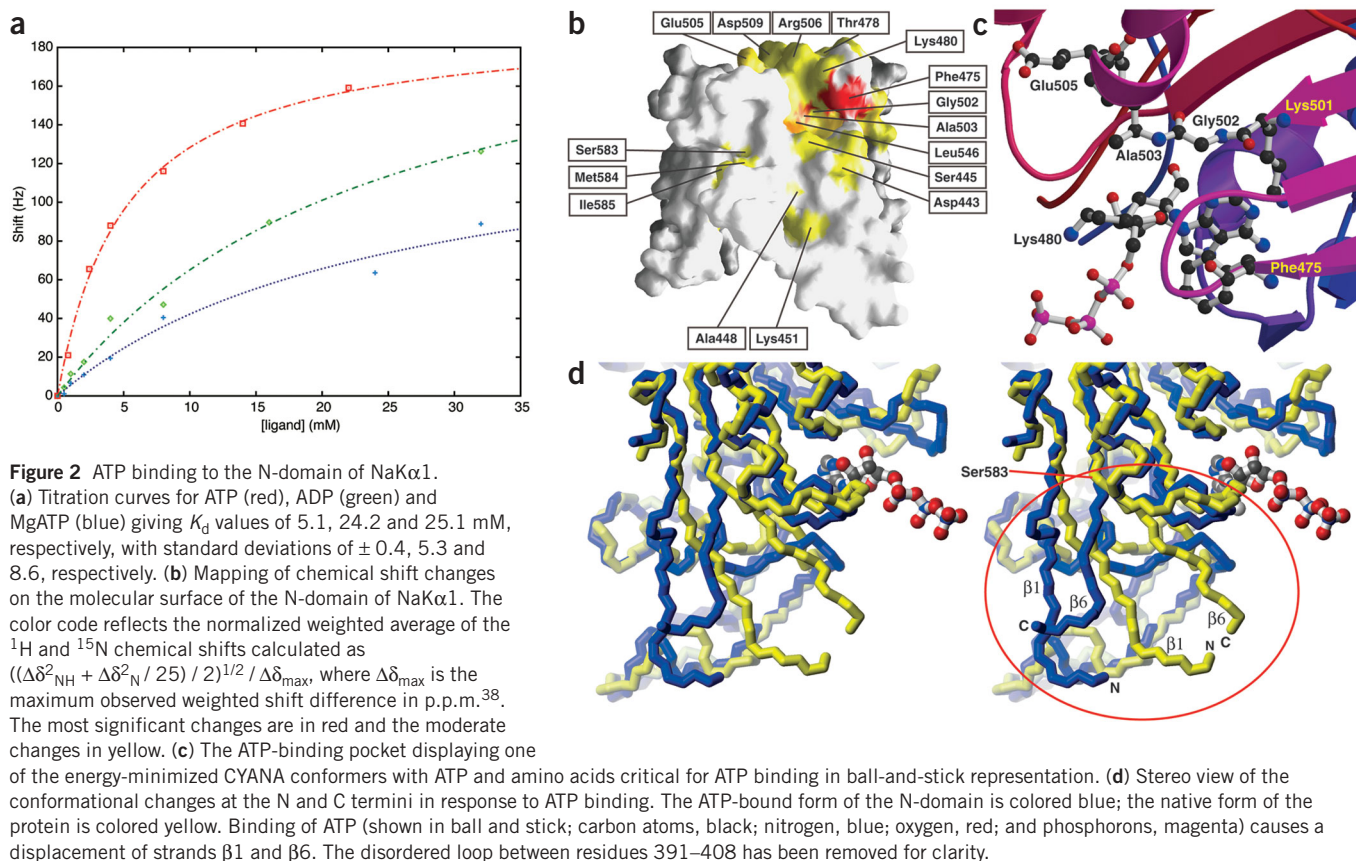
Figure 2 ATP binding to the N-domain of NaKα1. (**a**) Titration curves for ATP (red), ADP (green) and MgATP (blue) giving K_d values of 5.1, 24.2 and 25.1 mM, respectively, with standard deviations of ± 0.4, 5.3 and 8.6, respectively. (**b**) Mapping of chemical shift changes on the molecular surface of the N-domain of NaKα1. The color code reflects the normalized weighted average of the ^1H and ^{15}N chemical shifts calculated as $((\Delta\delta^2_{NH} + \Delta\delta^2_N / 25) / 2)^{1/2} / \Delta\delta_{max}$, where $\Delta\delta_{max}$ is the maximum observed weighted shift difference in p.p.m.[38]. The most significant changes are in red and the moderate changes in yellow. (**c**) The ATP-binding pocket displaying one of the energy-minimized CYANA conformers with ATP and amino acids critical for ATP binding in ball-and-stick representation. (**d**) Stereo view of the conformational changes at the N and C termini in response to ATP binding. The ATP-bound form of the N-domain is colored blue; the native form of the protein is colored yellow. Binding of ATP (shown in ball and stick; carbon atoms, black; nitrogen, blue; oxygen, red; and phosphorons, magenta) causes a displacement of strands β1 and β6. The disordered loop between residues 391–408 has been removed for clarity.

primarily responsible for the higher affinity of ATP compared with ADP. This idea is supported by ^{31}P NMR experiments in which the γ-phosphate shows a chemical shift difference of ~1 p.p.m. between the free and protein-bound forms of ATP, compared with ~0.2 p.p.m. for the β-phosphate group. The chemical shift changes caused by ATP binding may be a result of electrostatic interactions with the γ-phosphate, the extra negative charges relative to ADP or a conformational change in the binding pocket. Mapping of the spectral changes observed in the ATP titration onto the molecular surface of the N-domain revealed the location of the ATP-binding pocket (**Fig. 2b**). As expected from sequence comparison, the location of the nucleotide-binding site is identical in the NaKα1 and SERCA1a N-domains.

To determine the structure of the ATP–protein complex, we measured a series of NMR spectra under conditions where ATP binding was saturated by addition of an 11-fold excess of ATP over protein. The 25 ATP–protein distances that were derived from NOEs observed in the ω_1 ^{13}C-filtered/ω_2 ^{13}C-edited, as well as ^{13}C- and ^{15}N-edited NOESY spectra, allowed unambiguous determination of the position of ATP bound to the protein (**Figs. 1c** and **2c**). The nucleotide binds to the protein primarily through the base and sugar ring, leaving the phosphate groups exposed to solvent. The positioning of the base is determined by an extensive NOE network involving both the H2 and H8 protons. The sugar ring displays N-type puckering, consistent with the small $^3J_{H1'H2'}$ values observed for the bound ATP. NOEs to Phe475, Lys480, Ala503 and Leu546 firmly anchor the ribose ring to the protein. ATP binds to the N-domain of NaKα1 in the *anti* conformation, in contrast to the *syn* conformation seen in the 4-Å resolution complex of the Ca-ATPase with the inhibitor 2′,3′-O-(2,4,6-trinitrophenyl)-AMP[6]. It may be that the resolution of the X-ray structure does not permit unequivocal distinction between *syn* and *anti* conformation or that the bulky TNP group prevents the normal binding mode.

Superposition of the native structure of NaKα1 and the structure of SERCA1a shows that the arrangement of the crucial residues in the binding pocket is well preserved. In particular, the five residues that are strictly conserved in family II P-type ATPases, Lys501, Gly502, Ala503, Glu505 and Cys511, adopt similar orientations. Contributions to ATP binding originate from four different locations in the N-domain of NaKα1. Among these, only the highly conserved sequence 501-KGAPEXXXDRC-511 (where X is any amino acid) is well defined in the native form of the sodium pump, whereas the other three regions (Gly442–Glu446, Phe475–Lys480 and Gly542–Arg544) show a high degree of conformational variability. However, NOESY spectra of the complex showed many NOEs for Phe475–Lys480 that had not been observed previously in the native spectra, presumably as a result of changes in dynamic behavior.

The paucity of interactions found between the protein and ATP is in good agreement with the low binding constant (**Figs. 1c** and **2c**). The amino protons of the base form the only unambiguously identified hydrogen bond to Oε1 of Gln482. On the opposite side of the pocket, Phe475 provides a hydrophobic platform for a stacking interaction with the base of ATP. Mutation of the corresponding residue Phe487 in SERCA1a reduced the affinity for ATP by 22-fold[15]. Lys480 points into the binding pocket and is oriented toward the α-phosphate group of the nucleotide. Replacement of Lys480, however, had no effect in the sodium pump[16] and only a moderate effect on ATP binding in the calcium pump[15]. One possible explanation is that Arg506, which is absent in SERCA1a, could take over the function of Lys480 in NaKα1 when mutated. Mutational data[17,18] suggest that Arg544 is responsible for the stabilization of the γ- and/or
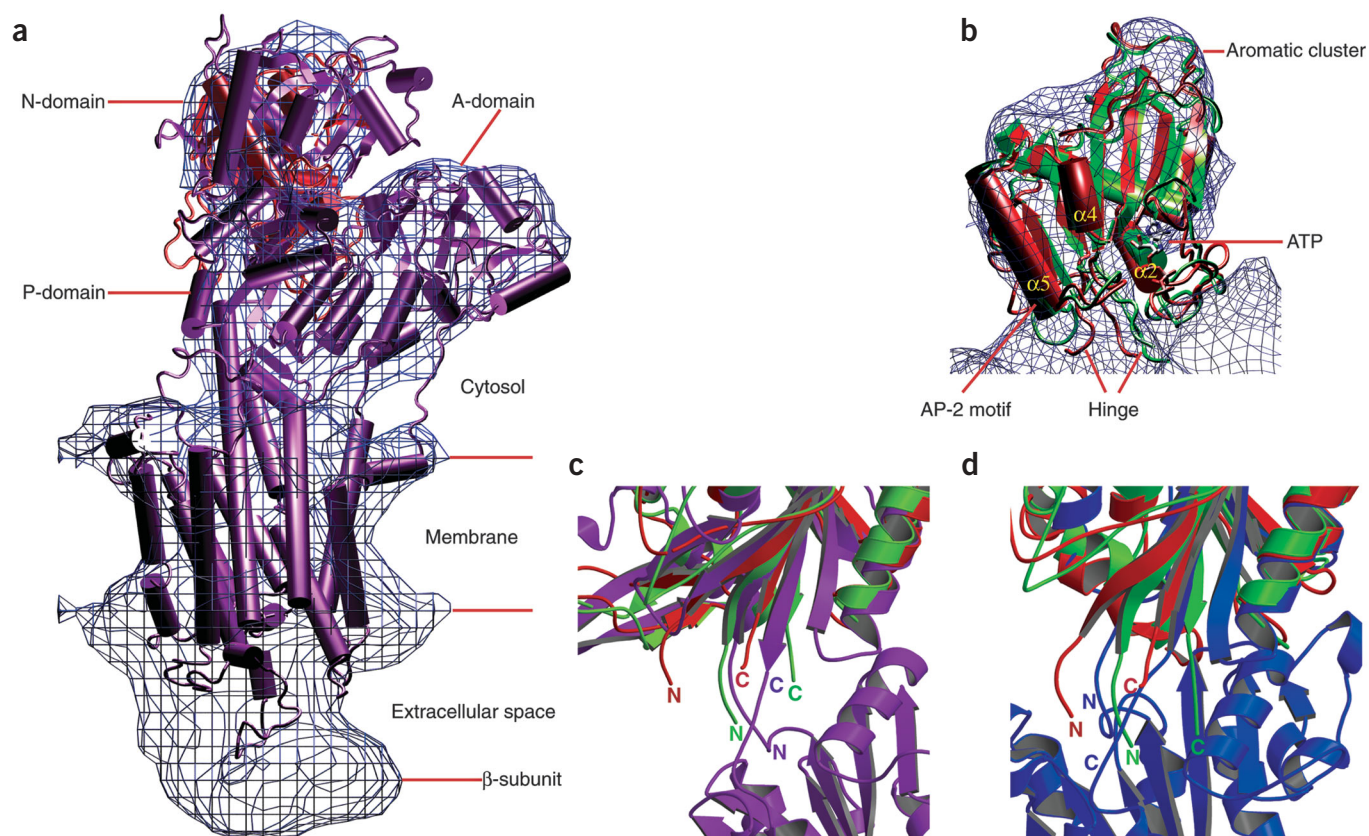
Figure 3 Docking and superposition of the native (green) and ATP-bound (red) N-domain of NaKα1, the E2(TG) form of Ca-ATPase (violet) and E1 form of H-ATPase (blue). (**a**) Solution structure of the ATP-bound N-domain of NaKα1 and the crystal structure of the E2(TG) form of SERCA1a docked in the 11-Å Cryo-EM structure of Na,K-ATPase illustrating the relative positions of the three cytosolic domains, the TM-domain and the β subunit, as well as the difference in positions of the N-domains. The surface corresponds to ~75% of the expected molecular volume. (**b**) Enlarged view of the native and ATP-bound N-domains of NaKα1. (**c**) Superposition of native and ATP-bound N-domain with the E2(TG) form of Ca-ATPase. (**d**) Superposition of native and ATP-bound N-domain with the model for the E1 form of H-ATPase. Panels **c** and **d** focus on residues in the hinge region between the N- and P-domains.

β-phosphate group of the substrate. Limited NOE data for the side chain of Arg544 are a result of its conformational variability in the ensemble of structures. However, Arg544 is well positioned to interact with either the γ- or the β-phosphate group or both. The observed ^{31}P chemical shift changes upon ATP titration with the N-domain of NaKα1 are indicative of direct interactions between the protein and these phosphates. In addition to these changes, differential line-broadening reduces the intensity of the downfield component of the γ-phosphate group by ~20%, presumably as a result of ^{31}P CSA/dipolar cross-correlation, thereby suggesting the proximity of ^{1}Hs of the protein to this phosphate group. However, because no direct restraints involving the phosphate groups were obtained, indications from the ^{31}P data are not reflected in the structures.

ATP-induced conformational changes

The X-ray structures of the Ca-ATPase show the N-domain to be an insertion within the P-domain. Two short, extended strands forming the N and C termini of the N-domain act as a hinge connecting the N- and P-domains. Superposition of the ensembles of native and ATP-bound proteins reveals a conformational difference in this hinge region of the isolated N-domain of NaKα1. Two lines of evidence indicate that the observed conformational change is significant within the context of the NMR structures. First, the differences between the two conformations are much larger than the conformational variability

within either ensemble of structures. The residues that form the hinge region are involved in 351 and 307 NOEs for the native and ATP-bound forms, respectively, which precisely define the conformation. Second, backbone dynamics measurements indicate that these residues all have {^{15}N-^{1}H}-NOE values >0.7 (data not shown), a value generally considered to define ordered structural elements. Taken together, these observations provide evidence that the hinge is a structured, integral part of the N-domain in both the native and ATP-bound forms, and not inherently 'flexible'.

In the structure of the native protein, strands β1 and β6 in the hinge region are bent, whereas the strands are straight in the ATP-bound form (**Fig. 2d**). Detailed analysis reveals that in the complex the carboxyl group of Ser583 is flipped ($\phi, \psi_{complex}$ = −79, 178° versus ϕ, ψ_{native} = 164, 57°) with respect to the native protein; consequently, residues 584–588 are rotated by ~40°. In both forms, strand β1 is oriented such that the secondary structure of the β-sheet is maintained. Additionally, the isolated loop region Arg423–Gly442 is displaced by ~5 Å between the two forms. The effect of ATP binding on the hinge region may be mediated by the flexible region of Gly542–Val545 or, more likely, through helix α2, given the extent of the chemical shift changes observed within this helix.

Relevance of the conformational changes

To test the biological relevance of the ATP-induced conformational changes observed for the isolated N-domain in context of the intact

Table 1 Experimental NMR data and structural statistics for the native and ATP-bound form of the N-domain of NaKα1[a]

	Native	ATP-bound
NOE upper distance limits		
Total	3,480	3,460
Long-range[b]	1,083	1,079
Intermolecular[c]	–	25
Torsion angle constraints	168	166
CYANA target function value ($Å^2$)	2.79	2.60
Distance constraint violations		
Number > 0.2 Å	0	0
Maximum (Å)	0.15	0.14
Torsion angle constraint violations		
Number > 2.5	4	2
Maximum (°)	4.1	4.0
AMBER energies (kcal mol^{-1})[d]		
Total	–6,831	–7,072
van der Waals	–618	–648
Electrostatic	–8,067	–8,327
R.m.s. deviation from ideal protein geometry		
Bond lengths (Å)	0.0077	0.0077
Bond angles (°)	2.07	2.04
Ramachandran plot analysis (all residues) (%)[e]		
Most favored regions	64	63
Additionally allowed regions	26	28
Generously allowed regions	7	6
Disallowed regions	3	4
R.m.s. deviation to the averaged coordinates (Å)		
N, Cα, C′ (379–391, 409–588)	0.97	1.00
All heavy atoms (379–391, 409–588)	1.40	1.46

[a]Average over the 20 energy-minimized conformers with the lowest CYANA target function values that represent the NMR solution structure. [b]Spanning five or more residues. [c]Between N-domain and ATP. [d]Ref. 28. [e]Using PROCHECK-NMR[31]

enzyme, we first docked the N-domain of NaKα1 and the E2(TG) form of SERCA1a (PDB entry 1IWO) into the electron density map of the 11-Å EM structure of Na,K-ATPase fixed in the E2 conformation[10] (**Fig. 3a,b**). Overall, the ensemble of solution structures of the Na,K-ATPase is reflected well by the EM structure (**Fig. 3b**). In particular, the region containing the aromatic cluster, which produced a poor fit with the same EM map for the E1[2Ca] form of Ca-ATPase[10], is now well positioned in the EM map. Poorly defined and mobile regions in the NMR structures lie outside the electron density. Both conformations of the hinge region lie within the EM electron density map (**Fig. 3b**). A global fit of the E2(TG) form of the Ca-ATPase X-ray structure to the Na,K-ATPase EM map demonstrates that the spatial relationship among the TM-, P- and A-domains is conserved, but the N-domain is slightly shifted. The Ca-ATPase, crystallized in the presence of thapsigargin, may be locked in the E2P or a related conformation, whereas the EM structure of Na,K-ATPase may resemble more closely the E2[2K] state. Alternatively, the discrepancy may also be a consequence of inherent, structural differences between Na,K- and Ca-ATPases.

Comparison of the E2(TG) structure of the Ca-ATPase with both the nucleotide-free and the ATP-bound forms of the N-domain of NaKα1 (**Fig. 3c**) indicates that the hinge region of the native form adopts a similar conformation, whereas the N- and C-termini of the ATP-bound form point in a different direction. In contrast, compari-

son with a model of the H-ATPase in the E1 form[19] (PDB entry 1MHS), which so far displays the shortest distance between the ATP-binding pocket and the invariant aspartate for any P-type ATPase structure, shows a close structural resemblance of the hinge region to the ATP-bound form of the N-domain of Na,K-ATPase (**Fig. 3d**). Although the reduced distance between the ATP-binding and phosphorylation sites makes sense, it remains intriguing that the model of the H-ATPase does not have the substrate ATP bound.

Interaction with other proteins

The N-domain of the Na,K-ATPase interacts with a number of proteins in either a direct or indirect way. Among these interactions, those with ankyrin and adaptor protein-2 (AP-2) are the most intensively studied. Ankyrin mediates the association to the spectrin-based cytoskeleton[20]—for example, in polarized epithelial cells—and thereby guarantees correct processing, targeting and transport of sodium pumps to the appropriate cellular compartment[21]. In NaKα1, one of the two ankyrin-binding motifs (448-ALLK-451) is located on the N-domain in helix α2, which is on the opposite face of the ATP-binding pocket. The motif displays only limited accessibility (**Fig. 1c**) and requires, at least partly, a displacement of residues Arg423–Gly442 to allow for an interaction with ankyrin.

The residues 535-YLEL-538 were identified as the motif required for dopamine-induced AP-2 binding in clathrin-dependent endocytosis of the Na,K-ATPase in renal epithelial cells[22]. This sequence is positioned at the end of the long helix α5, exposed on the surface (**Fig. 3b**). Tyr535, for which the Y535A mutation prevents AP-2 binding[22], performs an optimal hydrophobic stacking interaction with Phe531 and forms a hydrogen bond with Glu512. Although this mutation does not impair enzyme activity, it may destabilize helix α5 in such a way that the structural requirements for AP-2 binding are no longer met.

DISCUSSION

One of the most intriguing aspects of the P-type ATPases concerns the mechanism of the phosphotransfer reaction that drives the transport of ions. Comparison of the cytosolic domains of the E1[2Ca] and E2(TG) forms of Ca-ATPase reveals relatively few structural changes in the domains themselves. However, large differences for residues in the hinge regions between the N- and P-domains, as well as the A- and TM-domains, result in substantial domain movements. The conformational shifts within the hinge region of the isolated, soluble N-domain that we observed upon binding of ATP probably reflect similar changes in the interdomain hinge region of the intact enzyme. As the hinge of the isolated N-domain remains structured in solution, this distinct conformational change could therefore be part of the mechanism that relays the effects of ATP-binding in the intact enzyme.

The structure of the nucleotide-free N-domain of NaKα1 most likely corresponds to its conformation in the E2 state in the intact enzyme, in view of its similarity to the E2(TG) structure of the Ca-ATPase. Upon ATP binding, a shift towards the E1 state takes place. We speculate that in the intact enzyme, the effects of the conformational change that we observe for residues in the hinge region may be transmitted via the P-domain to the K$^+$-binding sites located in the membrane and/or cause the A-domain to disengage from the P-domain to facilitate the inclination of the N-domain onto the P-domain.

In the E2(TG) crystal structure of the Ca-ATPase, the ATP-binding site on the N-domain is located ~20 Å from the invariant Asp351. In the model of the H-ATPase in the E1 state, this distance is reduced to 15 Å, indicating that the (multiple) conformational changes that occur between these two states move the two sites closer together but are not by themselves sufficient to bring them into juxtaposition. It is likely

that, in analogy to the Ca-ATPase[6], binding of the Na^{+} ions induces the final inclination of the N-domain, allowing the γ-phosphate group to descend into the shallow cavity that harbors the invariant aspartate. We report that ATP binds the N-domain primarily via the sugar ring and base, while there is evidence that the γ-phosphate group also interacts with the protein. Although these interactions do not fully explain how the γ-phosphate stabilizes binding of ATP to the protein, our model allows the γ-phosphate the conformational freedom before phosphotransfer. Although our data do not solve the question of how the N-domain–bound ATP is brought into proximity of the invariant aspartate on the P-domain, they do provide experimental evidence that ATP-binding may actively trigger processes that precede the phosphorylation step essential for driving all P-type ATPases.

METHODS

Sample preparation. Residues 376–588 of the N-domain of NaKα1 were expressed in *Escherichia coli* strain BL21(DE3) (Novagen). Purification was facilitated by an N-terminal His-tag. Further purification and concentration of the protein was achieved with an UNO Q12 column (Bio-Rad). Details concerning expression, purification, sample preparation and the resonance assignment of the native and complex form of the N-domain will be reported elsewhere (M.H., G.S., P.G, S.M.G., J.P.A. & G.W.V., unpublished data).

NMR spectroscopy. The native and the ATP-bound NMR samples used for structure determination contained 2 mM protein in 20 mM Tris-HCl buffer, pH 8.6, prepared in H_2O/D_2O (95%/5%) with 0.02% (w/v) NaN_3 as a preservative. The ATP-bound samples also contained 22 mM ATP. ATP, ADP and MgATP titrations were recorded using 2 mM $^{13}C,^{15}N$-labeled or 0.5 mM ^{15}N-labeled samples. Changes in $[^1H,^{15}N]$ resonance position ($\Delta\delta$) were fit to the equation $\Delta\delta = \Delta\delta_{end} \times [\text{ligand}] / (K_d + [\text{ligand}])$, where $\Delta\delta_{end}$ denotes the resonance position at an infinite ligand concentration. NMR spectra were acquired at 22.7 °C on Varian Inova 600, 800 MHz and Bruker DRX600 spectrometers. Distance restraints for structure calculations were obtained from 3D-^{13}C-NOESY-HSQC and 3D-^{15}N-NOESY-HSQC spectra. In addition, 2D $^{13}C,^{15}N$-filtered NOESY and 3D ^{13}C-edited/$^{13}C,^{15}N$-filtered NOESY spectra were recorded on a NaKα1 sample containing a 0.67:1 ATP/protein molar ratio. All NOESY spectra were measured with an 80-ms NOE-mixing time. Stereospecific assignments of valine and leucine methyl groups were obtained by analysis of an $[^1H,^{13}C]$ CT-HSQC spectrum on a 10% ^{13}C-labeled sample[23]. All data were processed with NMRPipe[24].

Structure calculations. NOESY crosspeaks were picked and integrated in the aforementioned NOESY spectra using XEASY[25] and assigned using the automated NOESY crosspeak assignment method CANDID[26] in CYANA (http://www.guentert.com). The final structure calculations with CYANA were started from 200 conformers with random torsion angle values. Simulated annealing with 15,000 time steps per conformer was done with the DYANA torsion angle dynamics algorithm[27] in CYANA. Energy minimization of the 20 conformers with the lowest final target function values in a water shell using the AMBER force field[28] in OPALp[29] (**Table 1**) resulted in the solution structures of the N-domain of NaKα1 in the native and ATP-bound form. Statistical data indicative of the quality and completeness of the structure determination are listed in **Table 1**. The structures were validated using WHATIF[30] and PROCHECK-NMR[31]. Figures were generated with MOLMOL[32], MolScript[33], GRASP[34] and VMD[35].

Docking and modeling. Docking was done using the automated fitting procedure qrange in Situs 2.1 (ref. 36) for the ensemble of NMR structures of the N-domain of NaKα1 and the entire molecule, as well as the following substructures of the E2(TG) form of Ca-ATPase (PDB entry 1IWO): TM-domain (residues 59–112, 246–328 and 753–994); TM- and P-domains together (residues 59–112, 246–357 and 603–994); TM-, P- and N-domains (residues 59–112 and 246–994) and the TM-, P- and A-domains (residues 1–357 and 603–994). The resulting fitting coefficients were 0.435 for the entire molecule and 0.436, 0.448, 0.435 and 0.480 for the listed substructures, respectively.

Coordinates. The coordinates of the ensembles of the native and the complex structures of NaKα1 N-domain have been deposited in the Protein Data Bank (accession codes 1MO7 and 1MO8, respectively). Chemical shift data have been submitted to the BioMagResBank (accession codes 5576 and 5577, respectively).

1. Skou, J.C. The influence of some cations on an adenosine triphosphatase from peripheral nerves. *Biochim. Biophys. Acta* **23**, 394–401 (1957).
2. Horisberger, J.D., Lemas, V., Krähenbühl, J.P. & Rossier, B.C. Structure-function relationship of Na,K-ATPase. *Annu. Rev. Physiol.* **53**, 565–584 (1991).
3. Post, R.L, Hegyvary, C. & Kume, S. Activation by adenosine triphosphate in the phosphorylation kinetics of sodium and potassium ion transport adenosine triphosphatase. *J. Biol. Chem.* **247**, 6530–6540 (1972).
4. Jorgensen, J.R. & Pedersen, P.A. Role of phylogenetically conserved amino acids in folding of Na,K-ATPase. *Biochemistry* **40**, 7301–7308 (2001).
5. Kaplan, J.H. Biochemistry of Na,K-ATPase. *Annu. Rev. Biochem.* **71**, 511–535 (2002).
6. Toyoshima, C., Nakasako, M., Nomura, H. & Ogawa, H. Crystal structure of the calcium pump of sarcoplasmic reticulum at 2.6 Å resolution. *Nature* **405**, 647–655 (2000).
7. Toyoshima, C. & Nomura, H. Structural changes in the calcium pump accompanying the dissociation of calcium. *Nature* **418**, 605–611 (2002).
8. Zhang, P., Toyoshima, C., Yonekura, K., Green, N.M. & Stokes, D.L. Structure of the calcium pump from sarcoplasmic reticulum at 8-Å resolution. *Nature* **392**, 835–839 (1998).
9. Xu, C., Rice, W.J., He, W. & Stokes, D.L. A structural model for the catalytic cycle of Ca^{2+}-ATPase. *J. Mol. Biol.* **316**, 201–211 (2002).
10. Rice, W.J., Young, H.S., Martin, D.W., Sachs, J.R. & Stokes, D.L. Structure of Na^+,K^+-ATPase at 11-Å resolution: comparison with Ca^{2+}-ATPase in E_1 and E_2 states. *Biophys. J.* **80**, 2187–2197 (2001).
11. Hebert, H., Purhonen, P., Vorum, H., Thomsen, K. & Maunsbach, A.B. Three-dimensional structure of renal Na,K-ATPase from cryo-electron microscopy of two-dimensional crystals. *J. Mol. Biol.* **314**, 479–494 (2001).
12. Auer, M., Scarborough, G.A. & Kühlbrandt, W. Three-dimensional map of the plasma membrane H^+-ATPase in the open conformation. *Nature* **392**, 840–843 (1998).
13. Toyofuku, T., Kurzydlowski, K., Tada, M. & MacLennan, D.H. Amino acids Lys-Asp-Asp-Lys-Pro-Val402 in the Ca^{2+}-ATPase of cardiac sarcoplasmic reticulum are critical for functional association with phospholamban. *J. Biol. Chem.* **269**, 22929–22932 (1994).
14. Jorgensen, P.L & Pedersen, P.A. Structure-function relationships of Na^+, K^+, ATP, or Mg^{2+} binding and energy transduction in Na,K-ATPase. *Biochim. Biophys. Acta* **1505**, 57–74 (2001).
15. McIntosh, D.B., Woolley, D.G., Vilsen, B. & Andersen, J.P. Mutagenesis of segment ^{487}Phe-Ser-Arg-Asp-Arg-Lys^{492} of sarcoplasmic reticulum Ca^{2+}-ATPase produces pumps defective in ATP binding. *J. Biol. Chem.* **271**, 25778–25789 (1996).
16. Wang, K. & Farley, R.A. Lysine 480 is not an essential residue for ATP-binding or hydrolysis by Na,K-ATPase. *J. Biol. Chem.* **267**, 3577–3580 (1992).
17. Jacobsen, M.D., Pedersen, P.A. & Jorgensen, P.L. Importance of Na,K-ATPase residue α1-Arg^{544} in the segment Arg^{544}- Asp^{567} for high-affinity binding of ATP, ADP, or MgATP. *Biochemistry* **41**, 1451–1456 (2002).
18. Teramachi, S., Imagawa, T., Kaya, S. & Taniguchi, K. Replacement of several single amino acid side chains exposed to the inside of the ATP-binding pocket induces different extents of affinity change in the high and low affinity ATP-binding sites of rat Na/K-ATPase. *J. Biol. Chem.* **270**, 37394–37400 (2002).
19. Kühlbrandt, W., Zeelen, J. & Dietrich, J. Structure, mechanism, and regulation of the *Neurospora* plasma membrane H^+-ATPase. *Science* **297**, 1692–1696 (2002).
20. Jordan, C., Püschel, B., Koob, R. & Drenckhahn, D. Identification of a binding motif for ankyrin on the α-subunit of Na^+,K^+-ATPase. *J. Biol. Chem.* **270**, 29971–29975 (1995).
21. Therien, A.G. & Blostein, R. Mechanisms of sodium pump regulation. *Am. J. Physiol. Cell Physiol.* **279**, C541–566 (2000).
22. Doné, S.C. *et al.* Tyrosine 537 within the Na^+,K^+-ATPase α-subunit is essential for AP-2 binding and clathrin-dependent endocytosis. *J. Biol. Chem.* **277**, 17108–17111 (2002).
23. Neri, D., Szyperski, T., Otting, G., Senn, H. & Wüthrich, K. Stereospecific nuclear

magnetic resonance assignments of the methyl groups of valine and leucine in the DNA-binding domain of the 434 repressor by biosynthetically directed fractional ^{13}C labeling. *Biochemistry* **28**, 7510–7516 (1989).

24. Delaglio, F. *et al*. NMRPipe: a multidimensional spectral processing system based on UNIX pipes. *J. Biomol. NMR* **6**, 277–293 (1995).
25. Bartels, C., Xia, T.H., Billeter, M., Güntert, P. & Wüthrich, K. The program XEASY for computer-supported NMR spectral analysis of biological macromolecules. *J. Biomol. NMR* **6**, 1–10 (1995).
26. Herrmann, T., Güntert, P. & Wüthrich, K. Protein NMR structure determination with automated NOE assignment using the new software CANDID and the torsion angle dynamics algorithm DYANA. *J. Mol. Biol.* **319**, 209–227 (2002).
27. Güntert, P., Mumenthaler, C. & Wüthrich, K. Torsion angle dynamics for NMR structure calculation with the new program DYANA. *J. Mol. Biol.* **273**, 283–298 (1997).
28. Cornell, W.D. *et al*. A second generation force-field for the simulation of proteins, nucleic acids, and organic molecules. *J. Am. Chem. Soc.* **117**, 5179–5197 (1995).
29. Koradi, R., Billeter, M. & Güntert, P. Point-centered domain decomposition for parallel molecular dynamics simulation. *Comput. Phys. Commun.* **124**, 139–147 (2000).
30. Vriend, G. WHATIF: a molecular modeling and drug design program. *J. Mol. Graph.* **52**, 29–36 (1990).
31. Laskowski, R.A., Rullmann, J.A., MacArthur, M.W., Kaptein, R. & Thornton, J.M. AQUA and PROCHECK-NMR: programs for checking the quality of protein structures solved by NMR. *J. Biomol. NMR* **8**, 477–486 (1996).
32. Koradi, R., Billeter, M. & Wüthrich, K. MOLMOL: a program for display and analysis of macromolecular structures. *J. Mol. Graph.* **14**, 51–55 (1996).
33. Kraulis, P.J. MOLSCRIPT: a program to produce both detailed and schematic plots of protein structures. *J. Appl. Crystallogr.* **24**, 946–950 (1991).
34. Nicholls, A., Sharp, K. & Honig, B. Protein folding and association: insights from the interfacial and thermodynamic properties of hydrocarbons. *Proteins* **11**, 281–296 (1991).
35. Humphrey, W., Dalke, A. & Schulten, K. VMD—visual molecular dynamics. *J. Mol. Graph.* **14**, 33–38 (1996).
36. Wriggers, W., Milligan, R.A. & McCammon, J.A. Situs: a package for docking crystal structures into low-resolution maps from electron microscopy. *J. Struct. Biol.* **125**, 185–195 (1999).
37. Kleywegt, G.J. & Jones, T.A. A super position. *ESF/CCP4 Newslett.* **31**, 9–14 (1994).
38. Garrett, D.S., Seok, Y.J., Peterkofsky, A., Clore, G.M. & Gronenborn, A.M. Identification by NMR of the binding surface for the histidine-containing phospho-carrier protein HPr on the N-terminal domain of enzyme I of the *Escherichia coli* phosphotransferase system. *Biochemistry* **36**, 4393–4398 (1997).